

Photoproduction of Upsilon in Ultraperipheral Collisions at LHC Run2 energies

Dipanwita Dutta* and Ruchi Chudasama

Nuclear Physics Division, Bhabha Atomic Research Centre, Mumbai-400085, India

(Dated: October 31, 2021)

The exclusive Υ photoproduction in ultraperipheral proton-nucleus and nucleus-nucleus collisions at LHC energies is being investigated using pQCD framework which constrain the gluon distribution in the proton and nuclei at low x . Rapidity distributions of Υ photoproduction with different gluon distribution parameterization and gluon shadowing for nuclear PDFs including photon flux suppression for strong interaction, are being presented at LHC energies. Predictions done for ultraperipheral collisions at $\sqrt{s}=8.16$ TeV in pPb, and at $\sqrt{s}=5.02$ TeV in PbPb collisions which are LHC Run 2 Heavy Ion collision scenario and measurements of cross-section will be available soon.

I. INTRODUCTION

Ultraperipheral collisions (UPCs) of protons (ions) corresponds to the scenario when the impact parameter is larger than the sum of the radii of colliding hadron (ion), so that strong interaction is suppressed and they interact electromagnetically via emission of quasi-real photons. The large energies of the virtual photons produced in such reactions has stimulated many studies of photoproduction of heavy vector mesons (J/ψ and $\Upsilon(nS)$) [1–26], where large mass of the quarks provide a hard scale, justifying the use of factorization theorem of perturbative QCD (pQCD). Within leading logarithmic approximation of pQCD, the cross section of photoproduction of J/ψ or Υ is proportional to the square of gluon density of the target. As the fraction x of target momentum carried by the gluon is inversely proportional to the beam momentum, at LHC energies it is possible to explore the small x behavior of the gluon density in the proton and nuclei. In particular, it provides a sensitive tool to probe the onset of gluon saturation or nuclear gluon shadowing effects in small x .

Recently LHCb collaboration measured the yield of J/ψ and Υ [27, 28] at forward rapidities ($2 < y < 4.5$) in proton-proton UPC at 7, 8 TeV corresponds to x range for J/ψ , $6 \times 10^{-6} < x < 6 \times 10^{-5}$ and down to $x \sim 1.5 \times 10^{-5}$ for $\Upsilon(nS)$. Though J/ψ analysis confirmed the power law energy dependence of the $\gamma p \rightarrow J/\psi p$ cross section consistent with HERA results [29–31], but exclusive Υ measurement shows preference to the estimations including next-to-leading order calculation in contrast to HERA results of Υ photoproduction [32–34].

The ALICE collaboration measured the coherent J/ψ photoproduction [35, 36] in ultraperipheral collisions of PbPb at $\sqrt{s_{NN}} = 2.76$ TeV. The cross section was measured in two regions of the rapidity of produced J/ψ : $-3.6 < y < -2.6$ and at central rapidities $-0.9 < y < 0.9$ which corresponds to $x = 2 \times 10^{-2}$ and $x \sim 10^{-3}$ respectively. The results were compared with different model predictions and shows good agreement with models including nuclear gluon shadowing. ALICE also measured

J/ψ photoproduction [37] in pPb UPC at $\sqrt{s_{NN}} = 5.02$ TeV in the rapidity range $2.5 < y < 4$ (p-Pb) or $-3.6 < y < -2.6$ (Pb-p) corresponds to $x \sim 2 \times 10^{-2}$ and $\sim 2 \times 10^{-5}$ which didn't show significant change in the gluon density behavior of the proton between HERA and LHC energies.

CMS collaboration [38, 39] also measured $\Upsilon(1S)$ photoproduction cross section with pPb collisions at $\sqrt{s_{NN}} = 5.02$ TeV in the central rapidity range $-2.2 < y < 2.2$ corresponds to the Bjorken x value $1.3 \times 10^{-4} < x < 10^{-2}$. This result will provides the behavior of $\Upsilon(1S)$ photoproduction cross section with $W_{\gamma p}$, photon-proton center-of-mass energy, in the region between HERA [32–34] and LHCb [28] experiment.

The aim of the paper is the following. We estimate the Υ photoproduction in pPb collisions which is much preferable in comparison to proton-proton collision, due to asymmetric nature. Using the leading order (LO) pQCD, first we estimate of $\gamma p \rightarrow \Upsilon(nS)p$ and $\gamma Pb \rightarrow \Upsilon(nS)Pb$ employing different parameterization of the gluon distribution in the proton and nucleus and compare with the data of HERA and LHCb. Secondly, we calculate the rapidity distribution of exclusive Υ photoproduction in the proton-lead collisions for $\sqrt{s_{NN}} = 5.02$ TeV in the kinematic range of CMS experiment [40] and also done predictions in pPb UPC for $\sqrt{s_{NN}} = 8.16$ TeV which corresponds to the collision scenario of Run 2 LHC: data taken during Nov.-Dec. 2016. The suppression of photon flux due to strong interaction, which can reach up to $\sim 20\%$ difference in photon flux in forward rapidities [11] in proton-Pb UPC, is included by modifying the photon flux using the Glauber model of multiple proton-nucleus scattering. We also made predictions for the Υ photoproduction in PbPb UPC at $\sqrt{s_{NN}} = 5.02$ TeV, the scenario of LHC Run2 : data taken during Nov.-Dec. 2015, taking into account of recently available nuclear gluon shadowing parameterizations.

The paper is organized as follows. In section II, we discuss the photon flux generated by the proton and the nucleus. In section III, we discuss the photoproduction of $\Upsilon(1S)$ from proton with different gluon PDF and comparison with data. In section IV, we produce the results of photoproduction cross section of Υ with rapidity and discuss predictions for LHC Run 2.

* ddutta@barc.gov.in

II. PHOTON FLUX

The key ingredient of this study is the estimation of photon flux from proton and the lead nucleus. In case of proton-nucleus UPCs one needs to take into account the suppression of the flux due to the strong interaction between colliding particles. The photon flux of the proton (nucleus) of charge Z can be expressed as the convolution over the impact parameter b [11]:

$$N_{\gamma/Z}(\omega) = \int_0^\infty d^2\vec{b} \Gamma_{pA}(\vec{b}) N_{\gamma/Z}(\omega, \vec{b}), \quad (1)$$

where $N_{\gamma/Z}(\omega, \vec{b})$ is the photon flux in the transverse distance \vec{b} away from the proton (nucleus) [41],

$$N_{\gamma/Z}(\omega, \vec{b}) = C \left(\int_0^\infty dk_\perp \frac{k_\perp^2 F_Z(k_\perp^2 + \omega^2/\gamma_L^2)}{k_\perp^2 + \omega^2/\gamma_L^2} J_1(bk_\perp) \right)^2, \quad (2)$$

and $\Gamma_{pA}(\vec{b})$ is the probability to suppress the proton-nucleus strong interaction at small impact parameter b [11],

$$\Gamma_{pA}(\vec{b}) = \exp \left(-\sigma_{NN} \int_{-\infty}^\infty dz \rho_A(z, \vec{b}) \right). \quad (3)$$

In Eq. 2, $C = Z^2 \alpha_{em}/\pi^2$ where α_{em} is the fine structure constant, $F_Z(Q^2)$ is the charge form factor of the proton (nucleus), γ_L is the Lorentz factor ($\gamma_L = 2670, 4340$ for pPb at $\sqrt{s}_{NN} = 5.02, 8.16$ TeV, $\gamma_L = 3730, 6920, 7450$ for pp at $\sqrt{s} = 7, 13, 14$ TeV respectively and $\gamma_L = 2670$ for PbPb at $\sqrt{s}_{NN} = 5.02$ TeV), ω is the energy of the emitted photon and J_1 is the Bessel function of the first kind. In Eq. 3, σ_{NN} is the total nucleon-nucleon cross section and $\rho_A(\vec{r})$ is the nuclear density.

For $N_{\gamma/Z}(\omega)$ for the photon flux from the proton one generally use an approximate expression from Drees and Zeppenfeld [42],

$$N_{\gamma/p}(\omega) = \frac{\alpha_{em}}{2\pi} \left[1 + \left(1 - \frac{2\omega}{\sqrt{s}_{NN}} \right) \right] \left[\ln D - \frac{1}{6} + \frac{3}{D} - \frac{3}{2D^2} + \frac{1}{3D^3} \right]. \quad (4)$$

where $D = 1 + 0.71 \text{ GeV}^2 (\gamma_L^2/\omega^2)$. One also alternatively estimate the photon flux from the relativistic point like charge Z passing a target at a minimum impact parameter b_{min} :

$$N_{\gamma/Z}(\omega) = \frac{2Z^2 \alpha_{em}}{\pi} \left[\zeta K_0(\zeta) K_1(\zeta) - \frac{\zeta^2}{2} (K_1^2(\zeta) - K_0^2(\zeta)) \right] \quad (5)$$

where K_0 and K_1 are the modified Bessel functions of the second kind, $\zeta = \omega b_{min}/\gamma_L$, where b_{min} is the minimal admitted distance in the impact parameter space chosen to suppress the strong interaction and $b_{min} = 0.7$ fm for proton. In Fig. 1 we have compared the photon flux from the proton $N_{\gamma/p}$ for the Υ photoproduction, $pPb \rightarrow p + Pb + \Upsilon$, from the exact expression Eqs. 1-3

(presented by red curve) and the approximate DZ expression Eq. 4 (presented by black curve). The blue curve (referred as FF) is without SI suppression ($\Gamma_{pA}(b) = 1$ in Eq. 1). Upper panel shows photon flux for the pPb collisions at $\sqrt{s} = 5.02$ TeV, Pb towards +ve rapidity with $E_{Pb} = 1.58$ TeV and proton towards -ve rapidity with $E_p = 4$ TeV, $Pb + p \rightarrow Pb + p + \Upsilon$. Lower panel of Fig. 1 shows photon flux for pPb collisions at $\sqrt{s} = 8.16$ TeV, Pb towards +ve rapidity with $E_{Pb} = 2.56$ TeV and proton towards -ve rapidity with $E_p = 6.5$ TeV. It is observed that, the strong interaction between proton-nucleus reduce the photon flux substantially at large -ve rapidities (high photon energies).

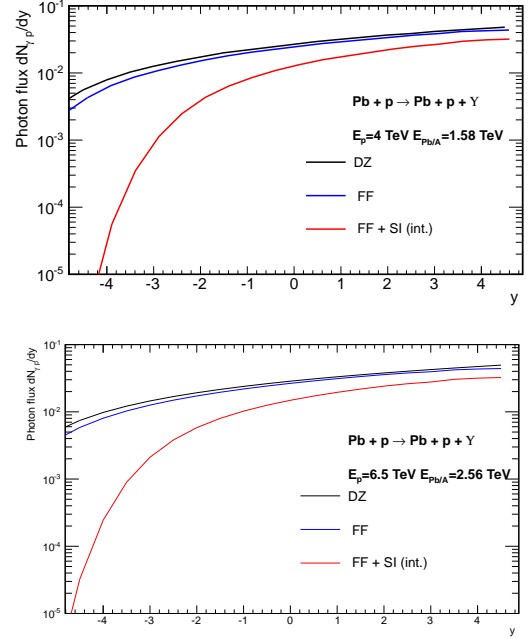


FIG. 1. The flux of photons from proton $N_{\gamma/p}$ as a function of Υ (1S) rapidity y in proton-Pb UPC. Upper panel shows photon flux for the pPb collisions at $\sqrt{s} = 5.02$ TeV, Pb towards +ve rapidity with $E_{Pb} = 1.58$ TeV and proton towards -ve rapidity with $E_p = 4$ TeV, $Pb + p \rightarrow Pb + p + \Upsilon$. Lower panel shows photon flux for pPb collisions at $\sqrt{s} = 8.16$ TeV, Pb towards +ve rapidity with $E_{Pb} = 2.56$ TeV and proton towards -ve rapidity with $E_p = 6.5$ TeV. DZ refers to Eq. 4, FF refers to $\Gamma_{pA}(b) = 1$ in Eq. 1.

Photon flux from nucleus can be similarly be estimated by using Eqs. 1-3 with appropriate nuclear charge form factor in Eq. 2. In this study, we preferred to use the point-like expression Eq. 5 for nucleus, following previous studies [10–13, 19–22], as the difference between the full calculation and point-like expression was observed to be insignificant for the photon flux from nucleus with $b_{min} = 1.15 R_{Pb}$ [11, 43]. For PbPb collisions we used the point-like charge expression for the photon flux for nucleus Eq. 5 with minimum impact parameter $b_{min} = 2R_{Pb}$.

III. PHOTOPRODUCTION OF Υ

The rapidity distribution of vector meson (Υ) production in proton-nucleus UPC interaction with proton from the right and nucleus from the left, is given by the sum of the two terms, each term in Weizsacker-Williams (WW) approximation [44, 45] is the product of photon flux and the cross-section of vector meson photoproduction:

$$\frac{\sigma_{AB \rightarrow AB\Upsilon}(y)}{dy} = N_{\gamma/A}(y)\sigma_{\gamma B \rightarrow \Upsilon B}(y) + N_{\gamma/B}(-y)\sigma_{\gamma A \rightarrow \Upsilon A}(-y) \quad (6)$$

Here $N_{\gamma/A(B)}(y)$ is the photon flux of proton or nucleus; $y = \ln(2\omega/M_\Upsilon)$ is the rapidity of Υ where ω is the photon energy and M_Υ is the mass of the Υ . The first term corresponds to photon from nucleus(A) while the second term is due to photon flux from proton(B). As the photon flux $\propto Z^2$ and have support only small value of ω , dying exponentially at large value of ω , the first term in r.h.s. (γp contribution) dominates and peaks at positive rapidity while the second term (γA contribution) peaks at negative rapidity.

The cross section of exclusive elastic photo-production of Υ on H ($H \equiv p, A$) can be written as

$$\sigma_{\gamma H \rightarrow \Upsilon H}(y) = \frac{d\sigma_{\gamma H \rightarrow \Upsilon H}}{dt} \Big|_{t=0} \int dt |F_H(t)|^2 \quad (7)$$

where $d\sigma_{\gamma H \rightarrow \Upsilon H}/dt|_{t=0}$ is the forward scattering amplitude and $F_H(t)$ is the charge form factor of the hadron (nucleus). Using leading order (LO) approximation, the scattering amplitude for elastic photoproduction of Υ from proton or a nucleus reads [11, 14]:

$$\frac{d\sigma_{\gamma H \rightarrow \Upsilon H}(W_{\gamma p}, t=0)}{dt} = \frac{M_\Upsilon^3 \Gamma_{ee} \pi^3}{48 \alpha_{e.m.} \mu^8} (1 + \eta^2) R_g^2 F^2(Q^2) [\alpha_s(Q^2) \frac{x G_H(x, Q^2)}{A}]^2 \quad (8)$$

where Γ_{ee} is the width of Υ electronic decay; α_{em} is the fine structure constant; $\alpha_s(Q^2)$ is the running strong coupling constant; $x = M_\Upsilon^2/W_{\gamma p}^2$, is the fraction of nucleon momentum carried by nucleons, $W_{\gamma p}$ is the γp center of mass energy; $G_H(x, Q^2)$ is the gluon distribution in the proton (nucleus) evaluated at momentum transfer $Q^2 = (M_\Upsilon/2)^2$. The relevant x region in CMS is $\approx 10^{-2} - 10^{-4}$ at central rapidities ($|y| < 2.4$). The factors $(1 + \eta^2)$, R_g^2 and $F^2(Q^2)$ corresponds to correction due to real part, skewness and next-to leading (NLO), respectively.

The t or the momentum-squared transferred dependence of the cross section for the proton target is generally parameterized in the form of rapidly decreasing exponential function, $e^{-B(W_{\gamma p})|t|}$, where the slope parameter $B(W_{\gamma p})$ depends weakly on energy. Here we use the Regge motivated expression for the slope parameter which is obtained from the fitting the data of exclusive J/ψ photoproduction [14], $B_\Upsilon(W_{\gamma p}) = 4.63 + 4.0 \times$

$0.06 \ln(W_{\gamma p}/90 \text{ GeV})$. Hence for proton, the photoproduction of Υ reads,

$$\sigma_{\gamma p \rightarrow \Upsilon p}(W_{\gamma p}) = \frac{1}{B(W_{\gamma p})} \frac{d\sigma_{\gamma p \rightarrow \Upsilon p}}{dt} \Big|_{t=0}. \quad (9)$$

To evaluate the factors η and R_g , we have fitted the shape of each gluon distribution $xG_T(x, Q^2) \propto 1/x^\lambda$ (details of gluon distributions used is given in next section) and determined the corresponding λ from the fit. The λ factors for $Q^2 = 22.4 \text{ GeV}^2$ (corresponds to $\Upsilon(1S)$) are given in Table I. The λ factors for CTEQ6L1(CTEQ6M) for $Q^2 = 25.1 \text{ GeV}^2$ and $Q^2 = 26.8 \text{ GeV}^2$ are 0.39(0.40) and 0.29(0.29) respectively. The factor η is evaluated using Gribov-Migdal relation [15, 46], $\eta = \tan(\pi\lambda/2)$. In collinear factorization for hard exclusive process, one should use gluon generalized parton distribution (GPD) and phenomenologically it is being treated by introducing enhancement factor R_g [11] given by,

$$R_g = \frac{2^{3+2\lambda} \Gamma(\frac{5}{2} + \lambda)}{\sqrt{\pi} \Gamma(4 + \lambda)} \quad (10)$$

The suppression factor $F^2(Q^2)$ contains all effects be-

TABLE I. The fitting factor for gluon PDFs λ .

Param.	MSTW08	CTEQ6L	CTEQ6L1	JMRTLO	CTEQ6M
λ	0.41	0.36	0.38	0.36	0.28

yond the leading order collinear factorization and discussed in Ref. [6, 47]. However this correction mainly influence the absolute normalization, but not the x dependence of the cross-section. We have used $F^2(Q^2) = 1$ and $Q^2 = M_\Upsilon^2/4$, which is the non-relativistic approximation that neglects the transverse momenta of b-quarks in the Υ wave function.

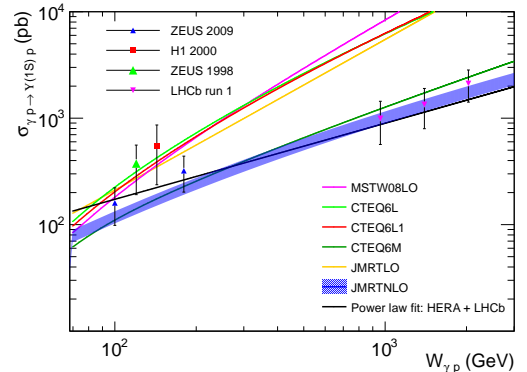


FIG. 2. Photoproduction cross section of $\Upsilon(1S)$, $\sigma_{\gamma p \rightarrow \Upsilon(1S)p}$ with photon-proton center of mass energy $W_{\gamma p}$ compared with the experimental data from HERA [32–34] and LHCb [28]. pQCD prediction with different gluon distribution compared with power law "Fit" to HERA + LHCb data.

A. Photoproduction of Υ from proton

Different parameterization of the gluon distribution in the proton are being used to estimate the photoproduction from $\sigma_{\gamma p \rightarrow \Upsilon(1S)p}$ and the results are shown in the Fig. 2. The LO pQCD estimation are being compared with HERA, LHCb data of exclusive photoproduction cross section of $\Upsilon(1S)$ with $W_{\gamma p}$. It also shows the power law fit to the data on $d\sigma_{\gamma p \rightarrow \Upsilon(1S)p}(W_{\gamma p}, t=0)/dt$ of HERA + LHCb and multiplied by the $B_{\Upsilon}(W_{\gamma p})$ using Eq. 9 to get the photoproduction cross section $\sigma_{\gamma p \rightarrow \Upsilon(1S)p}$. Gluon parameterization used are MSTW08 [48], CTEQ6L [49], CTEQ6L1 [49], JMRTO [14], CTEQ6M [49] and JMRTNLO [14]. Fig. 2 shows the LO pQCD predictions from Eqs. 8-9 at $Q^2 = M_{\Upsilon(1S)}^2/4$ for different gluon parameterization as discussed above. We have shown JMRTLO and JMRTNLO [14] cross-section of $\Upsilon(1S)$ photoproduction with $W_{\gamma p}$, for comparison and could not accomodate the error band for LO. The power law fit to HERA+LHCb data with $\delta = 0.76 \pm 0.27$ ($\sigma_{\gamma p \rightarrow \Upsilon(1S)p} \propto 1/B_{\Upsilon(1S)}(W_{\gamma p}) \times W_{\gamma p}^{\delta}$), shown by black curve, is less steep than LO predictions and comparable to NLO gluon PDFs, CTEQ6M and JMRTNLO predictions, the power law fit to which approximately gives $\delta = 0.84$.

B. Photoproduction of Υ from nucleus

In case of nuclear target, the photoproduction is given by,

$$\sigma_{\gamma A \rightarrow \Upsilon A}(W_{\gamma p}) = S_A^2(W_{\gamma p}) \frac{d\sigma_{\gamma p \rightarrow \Upsilon p}}{dt} \Big|_{t=0} \times \Phi_A(t_{\min}) \quad (11)$$

where

$$\Phi_A(t_{\min}) = \int_{t_{\min}}^{\infty} dt |F_A(t)|^2 \quad (12)$$

and $t_{\min} = -M_{\Upsilon}^4 m_N^2 / W_{\gamma p}^4$ is the minimal momentum transfer to the nucleus; $F_A(t)$ is the nuclear form factor which is given by the Fourier transform of the nuclear density distribution $F_A(t) = \int d^3r \rho(r) e^{i\mathbf{q} \cdot \mathbf{r}}$, where \mathbf{q} is the momentum transferred, $\rho(r)$ is the nuclear density approximated as modified hard sphere [50]. $S_A(W_{\gamma p})$ is the nuclear suppression factor given by,

$$S_A(W_{\gamma p}) = \frac{G_A(x, Q^2)}{AG_N(x, Q^2)} \times \left[\frac{(1 + \eta_A^2) R_{g,A}^2}{(1 + \eta^2) R_g^2} \right]^{1/2} \\ = R(x, Q^2) \times \kappa_{A/N}. \quad (13)$$

Here, $G_N(x, Q^2)$ and $G_A(x, Q^2)$ are the gluon density of nucleon and nucleus respectively; $R(x, Q^2)$ is the nuclear gluon modification factor. Due to nuclear gluon shadowing at small values of x , $G_A(x, Q^2) < AG_N(x, Q^2)$ and correspondingly $R(x, Q^2) < 1$. In addition, due to different growth of the nuclear gluon density $G_A(x, Q^2)$ with x

than free proton, $G_A(x, Q^2) \propto 1/x^{\lambda_A}$ where $\lambda_A < \lambda_p$ (λ_p corresponds to proton), results to the $\kappa_{A/N}$ factor [11].

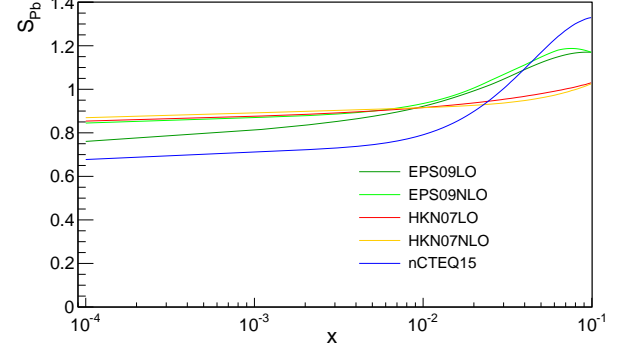


FIG. 3. Nuclear suppression factor of EPS09 [51] gluon distribution for $\Upsilon(1S)$, as defined in Eq. 13.

We have used gluon shadowing parameters from three recently available nuclear parton distribution functions: (i) EPS09 nuclear PDF at leading order and next-to-leading order [51] (ii) HKN07 at LO and NLO [52] (iii) nCTEQ15 [53] and estimated the suppression factor $S(W_{\gamma p})$ for $\Upsilon(1S, 2S, 3S)$ ($Q^2 = 22.4, 25.1, 26.8 \text{ GeV}^2$ for 1S, 2S and 3S respectively) in the low x region accessible in LHC experiments. We have used $\kappa_{A/N} = 0.87$ neglecting its variation with different gluon distributions [11]. Fig. 3 shows the variation of suppression factor of Pb nucleus S_{Pb} with x for $\Upsilon(1S)$ with three nuclear shadowing parameterizations. We should mention here that EPS09LO use CTEQ6L1 gluon distribution for free proton whereas EPS09NLO use CTEQ6M gluon PDF for proton. Hence results with CTEQ6L1(CTEQ6M) for γp and EPS09LO(EPS09NLO) for γPb , corresponds to the right combination of gluon distribution which are being compared with other combinations of gluon distributions for proton and nucleus.

IV. PHOTOPRODUCTION CROSS SECTION WITH RAPIDITY

We now present the results of photoproduction of $\Upsilon(1S)$ in the framework of leading-order QCD with two gluon exchange. Three factors, square of gluon distribution, photon flux and integrated nuclear form factor, determines the rapidity distribution of cross section.

A. Cross section for pPb collisions

Fig. 4 shows the rapidity distribution of the $\Upsilon(1S)$ photoproduction in proton-Pb UPC collisions integrated over momentum transfer t in the LHC kinematics as estimated by Eq. 6. Photon flux includes the effect of strong interaction suppression as discussed in Sections II. Here we used appropriate t dependence of cross section for

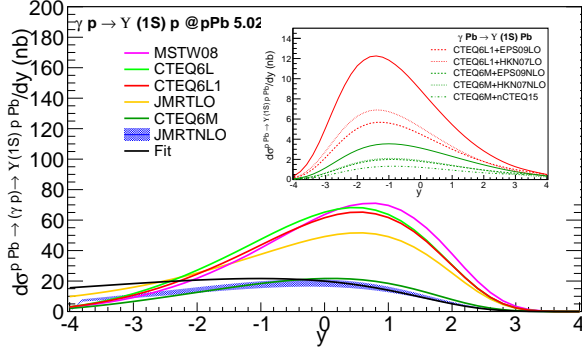


FIG. 4. The rapidity distribution of Υ (1S) photoproduction cross section for pPb collisions at $\sqrt{s} = 5.02$ TeV. The main and insert figure shows γp and γPb contributions respectively.

proton and nucleus as discussed in Sections III A and III B respectively. Figure shows the estimations using MSTW08 (magenta) [48], CTEQ6L (light green) [49], CTEQ6L1 (red) [49], CTEQ6M (dark green) [49], JMRTLO (orange) [14], JMRTNLO (blue) [?] gluon distribution functions and power law fit to HERA+LHCb data (black). Fig. 4, main figure, shows the $d\sigma/dy$ distribution for $pPb \rightarrow (\gamma p) \rightarrow \Upsilon(1S)pPb$, the dominant contribution, whereas insert figure shows the γPb contribution. Insert figure also shows the cross-section with different nuclear gluon shadowing parameterization (EPS09 [51], HKN07O [52] and nCTEQ15 [53]) for CTEQ6L1 and CTEQ6M gluon PDF of free proton. Solid lines show cross-section without shadowing whereas dashed curves are with nuclear gluon shadowing. HERA + LHCb power law fit (black), gives comparable description as of NLO gluon PDF, CTEQ6M.

TABLE II. Cross section of photoproduction of $\Upsilon(1S)$ at $\sqrt{s_{NN}} = 5.02$ TeV and at $\sqrt{s_{NN}} = 8.16$ TeV in pPb collisions in CMS acceptance $-2.4 < y < 2.4$ with different gluon PDF parameterizations.

Param.	$\sqrt{s}=5.02$ TeV			$\sqrt{s}=8.16$ TeV		
	γp	γPb	Total	γp	γPb	Total
MSTW08	229	42	271	488	82	570
CTEQ6L	229	40	269	451	73	524
CTEQ6L1	217	39	255	434	71	505
JMRTLO	182	32	214	360	59	419
CTEQ6M	77	13	90	127	19	146
JMRTNLO	69	11	80	115	17	132
Fit	85	14	99	122	18	140

We also estimate the $\Upsilon(1S)$ photoproduction cross-section for pPb collisions at $\sqrt{s_{NN}} = 8.16$ TeV, Run2 LHC collision scenario. Fig. 5 shows the $d\sigma/dy$ distribution for Υ (1S) for $\sqrt{s} = 8.16$ TeV. Similar to Fig. 4, main and insert figure of Fig. 5, shows γp and γPb contributions respectively. Table II gives the rapidity integrated cross section of Υ (1S) in CMS acceptance, i.e. $-2.4 < y < 2.4$ for $\sqrt{s} = 5.02$ TeV and $\sqrt{s} = 8.16$ TeV

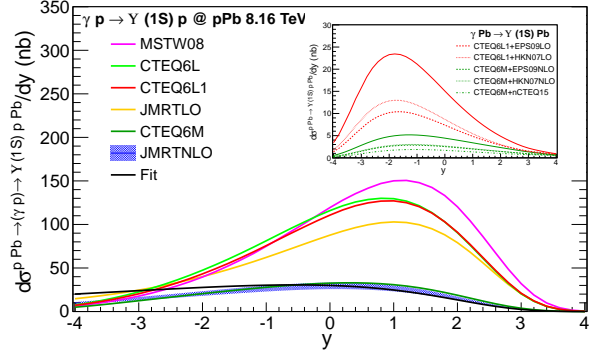


FIG. 5. The rapidity distribution of Υ (1S) photoproduction cross section for pPb collisions at $\sqrt{s} = 8.16$ TeV. The main and insert figure shows γp and γPb contributions respectively.

for different gluon PDF. We here present, the γp and γPb contributions to the Υ (1S) cross-section separately for different gluon PDF.

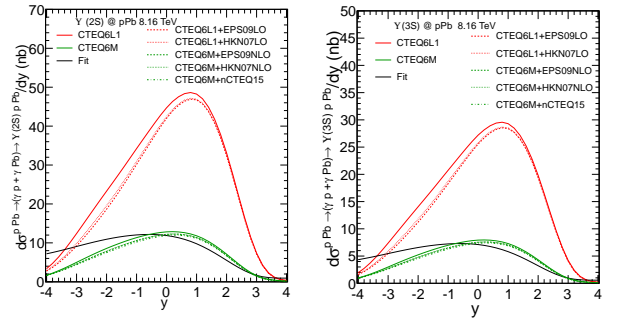


FIG. 6. The rapidity distribution of Υ (2S) (left plot) and Υ (3S) (right plot) photoproduction cross section for pPb collisions at $\sqrt{s} = 8.16$ TeV with different nuclear gluon shadowing parameterizations.

We also estimate the cross-section for Υ (2S) and Υ (3S) in pPb collisions at $\sqrt{s} = 8.16$ TeV. Fig. 6 shows the $d\sigma/dy$ distribution for Υ (2S) (left plot) and Υ (3S) (right plot) of total cross-section with different gluon shadowing parameterizations for CTEQ6L1 and CTEQ6M gluon PDF. Table III shows the cross-section for Υ (1S) at $\sqrt{s} = 5.02$ TeV and Υ (1S, 2S, 3S) at $\sqrt{s} = 8.16$ TeV pPb collisions with different nuclear gluon shadowing. Integrated cross-section for CMS acceptance and in full acceptance (numbers in bracket) with different nuclear gluon shadowing parameterizations are presented. Due to large photon flux from Pb nucleus, γp is the dominant part of the cross section, the γPb contribution is small and thus nuclear shadowing does not affect significantly the total $d\sigma/dy$ distribution as well as total integrated cross-section. We also estimate the ratio of cross-sections $\sigma^{\Upsilon(2S)}/\sigma^{\Upsilon(1S)}$ and $\sigma^{\Upsilon(3S)}/\sigma^{\Upsilon(1S)}$ for different gluon PDF in the rightmost two columns of Table III.

TABLE III. Cross section of photoproduction of $\Upsilon(1S)$ in pPb collisions at $\sqrt{s} = 5.02$ TeV and $\Upsilon(1S, 2S, 3S)$ in $\sqrt{s} = 8.16$ TeV in CMS acceptance $-2.4 < y < 2.4$ and also in full acceptance (numbers in bracket) with different nuclear gluon shadowing parameterizations. We also present the ratio of cross-section of $\sigma^{\Upsilon(2S)}/\sigma^{\Upsilon(1S)}$ and $\sigma^{\Upsilon(3S)}/\sigma^{\Upsilon(1S)}$.

Param.	5.02 TeV	8.16 TeV				
	$\sigma(\text{nb})$	$\sigma(\text{nb})$			Ratio	
	$\Upsilon(1S)$	$\Upsilon(1S)$	$\Upsilon(2S)$	$\Upsilon(3S)$	2S/1S	3S/1S
CTEQ6L1	255 (284)	505 (589)	178 (205)	108 (124)	0.35 (0.35)	0.21 (0.21)
EPS09LO	236 (260)	468 (538)	164 (188)	100 (113)	0.35 (0.35)	0.21 (0.21)
HKN07LO	239 (264)	474 (547)	167 (191)	101 (115)	0.35 (0.35)	0.21 (0.21)
CTEQ6M	90 (103)	146 (175)	50 (59)	31 (36)	0.34 (0.34)	0.21 (0.21)
EPS09NLO	84 (96)	138 (164)	47 (56)	29 (34)	0.34 (0.34)	0.21 (0.21)
HKN07NLO	85 (97)	138 (164)	47 (56)	29 (34)	0.34 (0.34)	0.21 (0.21)
nCTEQ15	82 (94)	134 (159)	46 (54)	28 (33)	0.34 (0.34)	0.21 (0.21)

B. Cross section for PbPb collisions

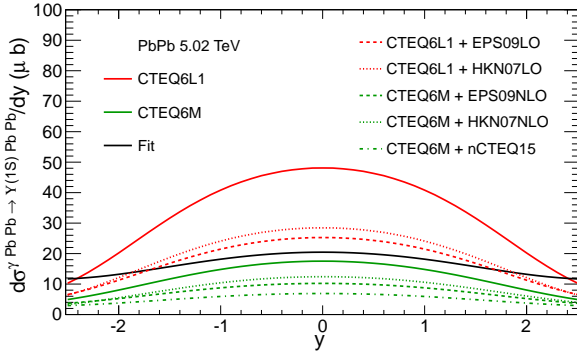


FIG. 7. The rapidity distribution of $\Upsilon(1S)$ photoproduction cross section for $PbPb$ collisions at $\sqrt{s_{NN}} = 5.02$ TeV. The solid graphs are cross section without nuclear shadowing and dashed graphs are with nuclear gluon shadowing parameters.

TABLE IV. Cross section of photoproduction of $\Upsilon(1S)$ in PbPb collisions at $\sqrt{s} = 5.02$ TeV in CMS acceptance $-2.4 < y < 2.4$ with different nuclear gluon shadowing parameterizations.

Param.	Gluon shadowing $\sigma(\mu\text{b})$			
	w/o shad.	EPS09LO	HKN07LO	
CTEQ6L1	166	89	99	
Fit	80	46	49	
	w/o shad.	EPS09NLO	HKN07NLO	nCTEQ15
CTEQ6M	62	37	38	26

The photoproduction of vector mesons in nucleus-

nucleus collisions is an important tool to study nuclear shadowing of gluon PDFs. In this section, we present results of $\Upsilon(1s)$ photoproduction cross section for PbPb UPC collisions at $\sqrt{s_{NN}} = 5.02$ TeV which is the LHC run 2 scenario. Fig. 7 shows the rapidity distribution of $\Upsilon(1s)$ photoproduction cross section, with different nuclear gluon shadowing. The solid graphs are cross section without nuclear shadowing and dashed graphs are with nuclear shadowing. Figure shows results with LO PDF and LO gluon shadowing from EPS09LO [51] and HKN07LO [52] and the results with NLO shadowing parameterizations from EPS09NLO [51], HKN07NLO [52] and nCTEQ15 [53]. It is noticed that, nuclear gluon shadowing, affects the cross section quite substantially for $\Upsilon(1S)$. It should be mentioned that, the measurement of J/ψ photoproduction cross section for PbPb UPC at 2.76 TeV by ALICE, satisfactorily [35, 36] reproduced by moderate gluon shadowing parameterizations from EPS09LO. Table IV gives the rapidity integrated $\Upsilon(1S)$ photoproduction cross section for CMS acceptance ($-2.4 < y < 2.4$) for PbPb UPC at $\sqrt{s} = 5.02$ TeV. The prediction of cross section from power law fit to HERA+LHCb data (referred as Fit in Table IV) is also quoted. The effect of shadowing is quite prominent in PbPb collisions at $\sqrt{s_{NN}} = 5.02$ TeV and cross-sections are reduced by 46%, 40% for CTEQ6L1 gluon PDF with EPS09LO and HKN07LO gluon shadowing respectively. The photoproduction cross-section for PbPb collisions with CTEQ6M free gluon PDF shows 40%, 39% and 58% reduction for EPS09NLO, HKN07NLO and nCTEQ15 nuclear gluon shadowing parameterizations, respectively.

Our results are also comparable with the earlier studies of $\Upsilon(1S)$ photoproduction. The cross section for pPb at $\sqrt{s_{NN}} = 5.02$ TeV, 236 nb with CTEQ6L1, is comparable with earlier estimation with EPS09 [20]. With NLO PDF CTEQ6M, the cross-section is 146 nb and from Fit 140 nb (see Table IV) at $\sqrt{s_{NN}} = 8.16$ TeV which is comparable to the value of $0.10 - 0.15 \mu\text{b}$ in Ref. [24] for IIM, bCGC and IP-SAT model predictions. The cross-sections are marginally different (6 – 7%) with gluon shadowing parameterizations at $\sqrt{s_{NN}} = 5.02$ TeV. The effect of shadowing is 7 – 8% in pPb collisions with $\sqrt{s_{NN}} = 8.16$ TeV. The cross-sections for PbPb collisions are also comparable to earlier predictions [10, 14, 18, 21, 22, 24–26, 43]. In our prediction, we have not considered NLO and other correction factors [14] which may reduce the cross-section and may be the possible inclusion in future.

V. CONCLUSIONS

In the present study, we have considered elastic photoproduction of $\Upsilon(nS)$ in ultraperipheral pPb and PbPb collisions at LHC. The photoproduction of vector meson is very useful to constrain the gluon modification, saturation or shadowing, due to the fact that, cross section is quadratically dependent on the gluon PDF. The predictions of pPb cross sections are consistent with HERA,

and LHCb data whereas future measurement will constrain about the gluon saturation in very low Bjorken x . The cross section of Upsilon photoproduction in PbPb UPC are found to be quite sensitive to gluon modifications and expect to extract information of nuclear shadowing.

ACKNOWLEDGMENTS

We would like to express our deepest thanks to Dr. A. K. Mohanty and Dr. David d'Enterria for fruitful discussions. We also acknowledge M. G. Ryskin, P. Jones, A. D. Martin and T. Teubner, as we used the plot of LO and NLO from Ref. [14, 38] for comparison and estimation of rapidity distribution.

-
- [1] A. J. Baltz, G. Baur, D. d'Enterria, L. Frankfurt, *et al.*, Phys. Rep. **458**, 1 (2008), arXiv:0706.3356 [nucl-ex].
 - [2] D. d'Enterria *et al.* (CMS Collaboration), J. Phys. G **35**, 104039 (2008), arXiv:0805.4769 [nucl-ex].
 - [3] S. J. Brodsky *et al.*, JETP **70**, 155 (1999), arXiv:hep-ph/9901229 [hep-ph].
 - [4] S. R. Klein and J. Nystrand, Phys. Rev. C **60**, 014903 (1999).
 - [5] S. R. Klein and J. Nystrand, Phys. Rev. Lett. **92**, 142003 (2004), arXiv:hep-ex/0311164 [hep-ph].
 - [6] L. Frankfurt, M. McDermott, and M. Strikman, JHEP **0103**, 045 (2001), arXiv:hep-ph/0009086 [hep-ph].
 - [7] M. Strikman, R. Vogt, and S. N. White, Phys. Rev. Lett. **96**, 082001 (2006), arXiv:hep-ph/0508296 [hep-ph].
 - [8] L. Motyka and G. Watt, Phys. Rev. D **78**, 014023 (2008).
 - [9] T. Lappi and H. Mantysaari, Phys. Rev. C **83**, 065202 (2011).
 - [10] T. Lappi and H. Mantysaari, Phys. Rev. C **87**, 032201 (2013).
 - [11] V. Guzey and M. Zhalov, JHEP **1402**, 46 (2014).
 - [12] V. Guzey and M. Zhalov, JHEP **1310**, 207 (2013).
 - [13] V. Guzey, E. Kryshnen, Strikman, and M. M., Zhalov, Phys. Lett. B **726**, 290 (2013).
 - [14] P. Jones, A. D. Martin, M. G. Ryskin, and T. Teubner, JHEP **1311**, 085 (2013), arXiv:1307.7099 [hep-ph].
 - [15] A. D. Martin, C. Nockles, M. G. Ryskin, and T. Teubner, Phys. Lett. B **662**, 252 (2008), arXiv:0709.4406 [hep-ph].
 - [16] V. A. Khoze, A. D. Martin, and M. G. Ryskin, Eur. Phys. J. C **18**, 167 (2000).
 - [17] L. A. Harland-Lang, V. A. Khoze, M. G. Ryskin, and W. J. Stirling, Eur. Phys. J. C **69**, 179 (2010).
 - [18] A. Adeluyi and C. A. Bertulani, Phys. Rev. C **85**, 044904 (2012), arXiv:1201.0146 [nucl-th].
 - [19] A. Adeluyi, C. A. Bertulani, and M. J. Murray, Phys. Rev. C **86**, 047901 (2012).
 - [20] A. Adeluyi and T. Nguyen, Phys. Rev. C **87**, 027901 (2013), arXiv:1302.4288 [nucl-th].
 - [21] G. Sampaio and M. V. T. Machado, Phys. Rev. C **89**, 025201 (2014).
 - [22] V. P. Goncalves, B. D. Moreira, and F. S. Navarra, Phys. Lett. B **742**, 172 (2015).
 - [23] V. P. Goncalves, L. S. Martins, and B. D. Moreira, Phys. Rev. D **96**, 074029 (2017), arXiv:1708.01498.
 - [24] V. P. Goncalves, M. V. T. Machado, B. D. Moreira, F. S. Navarra, and G. Sampaio, arXiv:1710.10070.
 - [25] G. Gil da Silveira and V. P. Goncalves, Phys. Rev. D **92**, 014013 (2015).
 - [26] G. Gil da Silveira, V. P. Goncalves, and M. M. Jaime, Phys. Rev. D **95**, 034020 (2017).
 - [27] R. Aaij *et al.* (LHCb Collaboration), J. Phys. G **41**, 055002 (2014).
 - [28] R. Aaij *et al.* (LHCb Collaboration), JHEP **1509**, 084 (2015).
 - [29] C. Adloff *et al.* (H1), Phys. Lett. B **483**, 23 (2000), arXiv:hep-ex/0003020 [hep-ex].
 - [30] A. Atkas *et al.* (H1), Eur. Phys. B **46**, 585 (2006), arXiv:hep-ex/0003020 [hep-ex].
 - [31] C. Alexa *et al.* (H1), Eur. Phys. J. C **73**, 2466 (2013), arXiv:1304.5162 [hep-ex].
 - [32] S. Chekanov *et al.* (ZEUS Collaboration), Phys. Lett. B **437**, 432 (1998).
 - [33] S. Chekanov *et al.* (ZEUS), Phys. Lett. B **680**, 4 (2009).
 - [34] S. Chekanov *et al.* (ZEUS), Phys. Lett. B **708**, 14 (2012).
 - [35] B. Abelev *et al.* (ALICE Collaboration), Phys. Lett. B **718**, 1273 (2013).
 - [36] E. Abbas *et al.* (ALICE Collaboration), Euro. Phys. J. C **73**, 2617 (2013).
 - [37] B. Abelev *et al.* (ALICE Collaboration), Phys. Rev. Lett. **113**, 232504 (2014).
 - [38] CMS Collaboration (CMS), CMS Physics Analysis Summary CMS-PAS-FSQ-13-009 (2013) <http://cdsweb.cern.ch/record/2147428>.
 - [39] R. Chudasama, D. Dutta, *et al.* (CMS collaboration), arXiv:1607.00786 [nucl-ex].
 - [40] S. Chatrchyan *et al.* (CMS), JINST **3**, S08004 (2008).
 - [41] M. Vidovic, M. Greiner, C. Best, and G. Soff, Phys. Rev. C **47**, 2308 (1993).
 - [42] M. Drees and D. Zeppenfeld, Phys. Rev. D **39**, 2536 (1989).
 - [43] V. Guzey and M. Klasen, arXiv:1603.06055 [hep-ph].
 - [44] C. F. v. Weizsacker, Z. Phys. **88**, 612 (1934).
 - [45] E. J. Williams, Phys. Rev. **45**, 729 (1934).
 - [46] V. N. Gribov and A. A. Migdal, Sov. J. Nuc. Phys. **8**, 583 (1969).
 - [47] M. G. Ryskin, R. Roberts, A. D. Martin, and E. M. Levin, Z. Phys. C **76**, 231 (1997).
 - [48] A. D. Martin, W. J. Stirling, R. S. Thorne, and G. Watt, Eur. Phys. C **63**, 189 (2009).
 - [49] J. Pumplin *et al.*, JHEP **07**, 012 (2002), arXiv:hep-ph/021195 [nucl-ex].
 - [50] A. Adeluyi and C. A. Bertulani, Phys. Rev. C **84**, 024916 (2011), arXiv:1104.4287 [nucl-th].
 - [51] E. J. Eskola, H. Paukkunen, and C. A. Salgado, JHEP **0904**, 065 (2009), arXiv:0902.4154 [hep-ph].
 - [52] M. Hirai *et al.*, Phys. Rev. C **76**, 065207 (2007).
 - [53] K. Kovarik *et al.*, arXiv:1509.00792 [hep-ph].